

# Temperature dependence of Mott transition in VO<sub>2</sub> and programmable critical temperature sensor

Bong-Jun Kim\*, Yong Wook Lee, Byung-Gyu Chae, Sun Jin Yun, Soo-Young Oh, and Hyun-Tak Kim  
*IT Convergence Components Lab., ETRI, Daejeon 305-350, Republic of Korea*

Yong-Sik Lim

*Department of Applied Physics, Konkuk University, Chungju, Chungbuk 380-701, Republic of Korea*

The temperature dependence of the Mott metal-insulator transition (MIT) is studied with a VO<sub>2</sub>-based two-terminal device. When a constant voltage is applied to the device, an abrupt current jump is observed with temperature. With increasing applied voltages, the transition temperature of the MIT current jump decreases. We find a monoclinic and electronically correlated metal (MCM) phase between the abrupt current jump and the structural phase transition (SPT). After the transition from insulator to metal, a linear increase in current (or conductivity) is shown with temperature until the current becomes a constant maximum value above  $T_{SPT} \approx 68^\circ\text{C}$ . The SPT is confirmed by micro-Raman spectroscopy measurements. Optical microscopy analysis reveals the absence of the local current path in micro scale in the VO<sub>2</sub> device. The current uniformly flows throughout the surface of the VO<sub>2</sub> film when the MIT occurs. This device can be used as a programmable critical temperature sensor. PACS numbers: 71.27.+a, 71.30.+h

The first-order Mott discontinuous metal-insulator transition (MIT) has been studied as a function of temperature in numerous materials such as Ti<sub>2</sub>O<sub>3</sub>, V<sub>2</sub>O<sub>3</sub>, and VO<sub>2</sub> etc [1]. Almost all have a transition temperature,  $T_{MIT}$ , below room temperature except VO<sub>2</sub> which has  $T_{MIT} \approx 68^\circ\text{C}$ . In particular, VO<sub>2</sub> thin films were used for fabrication of two- and three-terminal devices controlled by an electric field [2]. A high-speed Mott switching device using an abrupt current jump as observed in I-V measurements was predicted for manufacturing in the nano-level transistor regime [3,4].

Moreover, Raman experiments [5] for a VO<sub>2</sub> film have showed monoclinic-insulator peaks after the film had undergone an electric-field-induced transition from an insulator to a metal. Furthermore, tetragonal-metal peaks have been associated with the structural phase transition (SPT) above  $68^\circ\text{C}$ . Also no evidence of phonon softening near the transition temperature has been found by the temperature dependence of Raman spectra measured with a VO<sub>2</sub> single crystal and a thin film [6]. These results support the electron correlation model of the MIT. However, some reports argue that the electric field-induced MIT is due to Joule heating by current and is accompanied by SPT, and that, furthermore, the local current path or current filament formed by the dielectric breakdown [7] can also cause the jump (MIT). The dielectric breakdown was described by depinning and the collective transport of charge carriers above a threshold voltage. Here, we try to elucidate this ambiguity through the analysis of our present research.

Another interesting aspect in VO<sub>2</sub> is that the  $T_{MIT}$  can be modified by doping [8,9] and stress [10]. VO<sub>2</sub> thin films deposited on (001) and (110) TiO<sub>2</sub> substrates showed a modified  $T_{MIT}$  of 27 and  $96^\circ\text{C}$ , respectively, where the c-axis length was stressed by a lattice mis-

match between the film and the substrate [10]. The modification of the  $T_{MIT}$  by doping and stress is restricted to within a fixed temperature, whereas the  $T_{MIT}$  induced by an electric field linearly depends on the electric field intensity.

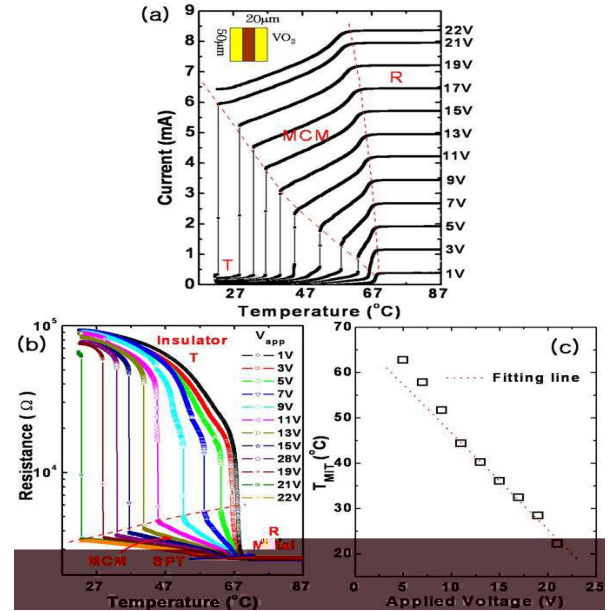


FIG. 1. Temperature dependences of, (a) the current, and (b) the resistance for the MIT (Jump) at applied voltages. The transition temperatures of the MIT shift towards room temperature with increasing applied voltages. An intermediate monoclinic and correlated metal (MCM) phase is located between red-dotted lines. Fig. (b) is plotted from  $R=V/I$  in I-T curves of Fig. 1(a). Fig. (c) The applied voltage dependence of  $T_{MIT}$  from fig. (a). Dotted line is a fit to a linear function. The slope of a fitting line is  $-2.13^\circ\text{C}/\text{Volt}$ .

In this letter, for applications of the MIT over wide temperature ranges, we observe a modification of the  $T_{MIT}$  in a  $\text{VO}_2$  thin film device by applying voltages. Actually, the modification of the  $T_{MIT}$  is appreciable for a critical temperature sensor working at any set temperature below  $68^\circ\text{C}$ . The relation between the MIT and the SPT is investigated by micro-Raman spectroscopy. By analysis of the micro-scale current localization with optical microscopy, we confirm a uniform current flow that is not explained by dielectric breakdown. Moreover, we perform a switching experiment with a triangle wave to observe generation of Joule heat in a device.

$\text{VO}_2$  films on  $(10\bar{1}0)$   $\text{Al}_2\text{O}_3$  substrates have been prepared by the sol-gel method described in detail elsewhere [11]. In order to observe the temperature dependence of the MIT,  $\text{VO}_2$ -based two-terminal devices were fabricated in which  $\text{VO}_2$  films were ion-milled with an  $\text{Ar}^+$  beam. The thickness of the  $\text{VO}_2$  films is about 100 nm. Nickel was used as an electrode metal for the Ohmic contacts. The fabricated devices have a channel width of  $W=50\text{ }\mu\text{m}$  and a channel length between electrodes of  $L=20\text{ }\mu\text{m}$ . The temperature dependence of the current was measured from room temperature to 450 K in a cryostat. The I-V characteristics of the devices were measured by a precision semiconductor parameter analyzer (HP4156B). As observed in the I-V measurements, the MIT occurs around 22 V at room temperature. Thus constant voltages are applied in the range from 1 to 22 V.

Raman spectra were measured with an Ar laser beam to which the  $\text{VO}_2$  film between the electrodes was exposed. The 514.5 nm line of an  $\text{Ar}^+$  laser at a power of 4.5 mW was employed in a micro-Raman (LABRAM 300) with a spectral resolution less than  $2\text{ cm}^{-1}$ . The Raman system was also equipped with an Olympus microscope (BX41) which allowed accurate alignment of the beam onto the device. During the Raman measurement, the current applied to the device after the abrupt MIT was limited to the compliance (restricted) current to prevent any possible damage in the device due to excess current. The Raman spectrum measurement took 60 sec.

Figure 1(a) shows the current-voltage curves measured by a  $\text{VO}_2$  device with  $V_{MIT} \approx 21\text{ V}$  (inset figure) as a function of temperature for various constant applied voltages. At  $V_{applied} = 1\text{ V}$ , the resistance behavior with the temperature is typical of a curve with the MIT near  $68^\circ\text{C}$  (Fig. 1b). Above  $68^\circ\text{C}$ , currents have a constant value of 0.38 mA. As the constant applied voltage is increased from 1 to 22 V, an abrupt current jump clearly appear above 5 V. The transition temperatures gradually shift from  $68^\circ\text{C}$  at  $V_{applied} = 1\text{ V}$  to room temperature at  $V_{applied} = 21\text{ V}$ . After an abrupt current jump occurred in the electric field,  $\text{VO}_2$  devices showed the Ohmic behaviors in our previous research [2]. Moreover, we clearly found a new region of linear behavior of current in the I-T curves. The region corresponds to

an intermediate regime between abrupt current jumps and a red-dash line which is the SPT line confirmed by micro-Raman measurements shown in the next section. Thus we divided the I-T curves into three phases, the semiconductor-monoclinic transient triclinic T phase, the intermediate phase and the tetragonal rutile R metal phase. The SPT temperatures decrease slightly with increasing applied voltage due to increase of Joule heat.

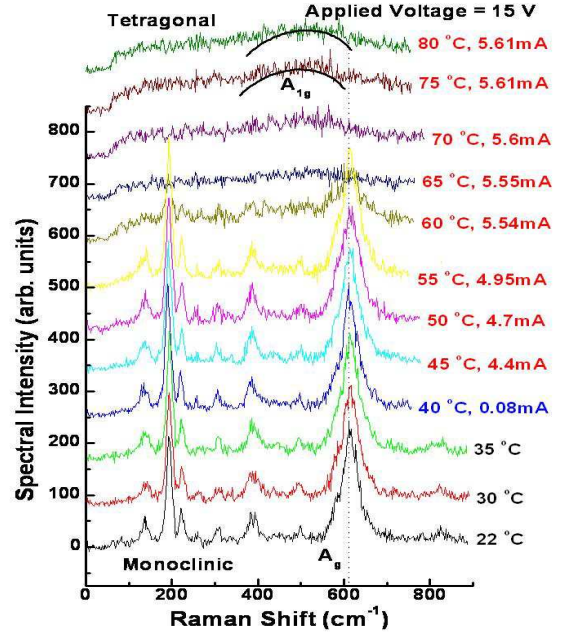


FIG. 2. Temperature dependence of Raman peaks at 15 V. The monoclinic  $A_g$  peak at  $617\text{ cm}^{-1}$  disappears around  $65^\circ\text{C}$ . Above  $70^\circ\text{C}$ , the tetragonal  $A_{1g}$  peak appears and is overlaid with solid lines.

Figure 1(b) shows the resistances as a function of temperature at constant applied voltages and are plotted on a log scale. Resistances were obtained from  $R=V/I$  in Fig. 1(a). In the intermediate phase between the dashed lines in fig. 1(a), the current linearly increases with increasing temperature, whereas in this region the resistance gradually decreases (the conductivity increases) at each applied voltages, as shown in Fig. 1(b). This strongly suggests that  $\text{VO}_2$  is in a metallic state different from the tetragonal metallic state because the temperature is still less than  $68^\circ\text{C}$ . Near the SPT, the resistance becomes a minimum and the conductivity ( $\sigma \propto 1/R$ ) has a maximum value.

In a strongly correlated system, the electrical conductivity is proportional to square of the effective mass between quasiparticles;  $\sigma \propto (m^*/m)^2$  where  $m^*/m = 1/(1 - (U/U_c)^2)$  for an inhomogeneous system and  $U$  is the on-site Coulomb correlation energy between quasiparticles [12–14]. Therefore, since the intermediate phase has the maximum conductivity near  $T_{SPT}$ , it is regarded as the intermediate phase being strongly correlated; the

intermediate phase is named as a monoclinic and correlated metal (MCM) phase. The MCM phase arises from inhomogeneity [13,14].

The MCM phase is described by the equation  $n_c(T, E) = n(E) + n(T)$ , where  $n(E)$  is the hole density excited by an electric field (voltage),  $n(T)$  is the hole density excited by temperature, and  $n_c(T, E)$  is the critical hole density in which the MIT occurs due to the electric field and temperature excitations [2]. Hole carriers were confirmed by Hall measurement [2]. For constant  $n_c$ ,  $n(T)$  decreases, and  $T_{MIT}$  decreases as  $n(E)$  increases, which suggests that the MIT is controlled by doped holes.

Figure 1(c) shows the applied voltage dependence of  $T_{MIT}$  fitting to a linear function;  $T_{MIT} = -2.13V_{applied} + 68$ . This fitting line is denoted as a dotted line. At  $V_{applied} = 0$ ,  $T_{MIT} = 68^\circ\text{C}$ , which is the SPT temperature. Except for a deviation of the fitting near  $68^\circ\text{C}$ ,  $T_{MIT}$  follows the linear. This indicates that the device can be used as a programmable critical temperature sensor.

Figure 2 shows temperature dependence of Raman peaks and currents simultaneously measured by applying 15 V to the device. The Raman peaks are measured at a low laser power which was decreased by using neutral density (ND) filter with an optical density of  $D=2$ , which does not make a local laser beam spot visible on the film (see next section). In the temperature range from 22 to  $40^\circ\text{C}$ , the intense monoclinic  $A_g$  peaks near 193 and  $617\text{ cm}^{-1}$  appear in accordance with our previous Raman experiments. At  $45^\circ\text{C}$ , no clear changes occur in the Raman curve, nevertheless, the MIT occurred between 40 and  $45^\circ\text{C}$  with a current jump from 0.08 to 4.4 mA. This indicates that the MIT occurs without the SPT. Monoclinic  $A_g$  peaks are still visible up to  $60^\circ\text{C}$  with little decrease in intensity.  $A_g$  peaks disappear around  $65^\circ\text{C}$  and the broad tetragonal  $A_{1g}$  peak then appears near  $550\text{ cm}^{-1}$ . This indicates the SPT from monoclinic to rutile tetragonal structure. Above  $65^\circ\text{C}$ , the current has a constant value of 5.61 mA, as a constant current is shown in the R region of Fig. 1(a). Thus the dotted red line between MCM and R in Fig. 1(a) is regarded as the SPT. Note that a difference between  $T_{MIT} \approx 37^\circ\text{C}$  at 15 V in Fig. 1(a) and  $T_{MIT} \approx 45^\circ\text{C}$  in Fig. 2 may be due to different measurement environments in I-V and Raman spectroscopy.

We investigated changes of surface color and surface status of  $\text{VO}_2$  by the applied voltages and a laser beam with the variable temperature. Figure 3(a) shows an optical image of the  $\text{VO}_2$  device taken at 10 V and  $60^\circ\text{C}$ , in which ND filter was not used. The dark trace of the laser spot in a dashed circle appears on  $\text{VO}_2$  film. The temperature of the film in the laser spot is higher than  $68^\circ\text{C}$  showing the difference of the reflectance with another part in the film. At 10 V and  $70^\circ\text{C}$ , laser beam spot is no longer visible, as shown in Fig. 3(b). The contrast

of  $\text{VO}_2$  film is changed only by the temperature. Thus the optical image shows that the current flows uniformly on the  $\text{VO}_2$  film by applied voltage.

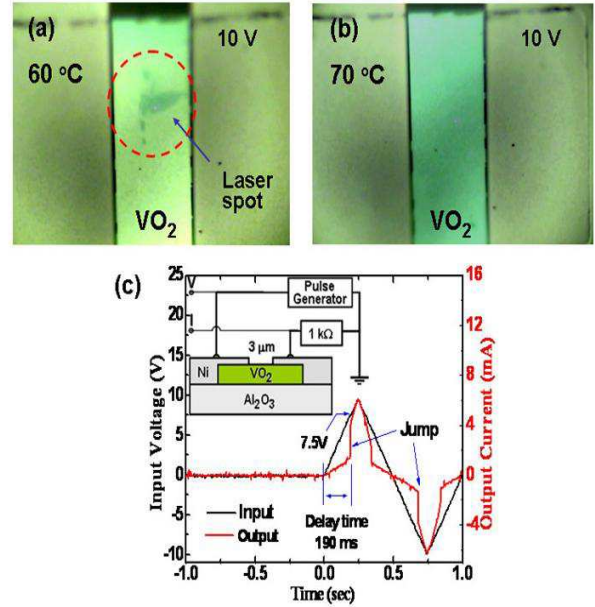


FIG. 3. (a) Enlarged images of a  $\text{VO}_2$  device taken by optical microscopy. At a high laser power without a ND filter, a local laser spot appears at  $60^\circ\text{C}$  and 10 V. (b) At  $70^\circ\text{C}$  and 10 V, the laser spot is no longer visible. The  $\text{VO}_2$  films are then in the metal phase. (c) For a  $\text{VO}_2$  device with  $L=3\text{ }\mu\text{m}$ ,  $W=10\text{ }\mu\text{m}$ . The MIT is switched repeatedly at 7.5 V (red solid line). The output current (red right axis) is measured for an input triangle voltage (black solid line) of 1 Hz (left axis). Delay time  $\tau$  took 190 msec.  $V_{MIT}=7.5\text{ V}$  and  $I_{MIT}=4\text{ mA}$  were obtained. Inset shows the measurement circuit.

From optical measurements, the transition time of the MIT in  $\text{VO}_2$  has been measured to be in the subpicosecond regime [15,16] and in the order of nanosecond for an electronic device [17]. The heating model predicts that a delay time takes about  $1\text{ }\mu\text{sec}$  for a device with  $L=3\text{ }\mu\text{m}$  and  $W=50\text{ }\mu\text{m}$  to become  $T_d = T_{SPT}$  where  $T_d$  is a device temperature in a previous research [17]. In order to check whether the SPT is produced by Joule heating or not ( $Q = \int_0^\tau IV dt$ , where  $\tau \approx 190\text{ msec}$  which is a long delay time to  $1\text{ }\mu\text{sec}$ ;  $Q$  increases with increase of  $\tau$ ), one triangle wave with a period of 1 sec is applied to a device with a width of  $L=3\text{ }\mu\text{m}$  and a length of  $W=10\text{ }\mu\text{m}$ , which has  $V_{MIT} = 7.5\text{ V}$  (Fig. 3(c)). The MIT is shown as a jump at  $V_{MIT} \approx 7.5\text{ V}$  and  $I_{MIT} \approx 4\text{ mA}$ . This indicates that  $T_d$  produced by Joule heating is less than  $T_{SPT}$ . When  $T_d > T_{SPT}$ , the current jump should not be observed because the MIT as observed in the I-V curves is continuous without jump above  $T_{SPT}$  (Fig. 1(b)). Thus Joule heat does not increase  $T_d$  up to  $T_{SPT}$ , which indicates that Joule heat is not a cause of the MIT.

In conclusion, the  $\text{VO}_2$ -based devices show the separa-

tion of the MIT from the SPT. The  $T_{MIT}$  is controlled by the applied voltage, a filament for a conducting path is not formed and the large Joule heat which causes the SPT is not produced even in the high current induced by the MIT. In future, this device can be utilized as a programmable critical temperature or infrared sensor and was named MoBRiK [14].

---

\* bjkim@etri.re.kr

- [1] N. F. Mott 1990 *Metal – Insulator Transition* (Taylor and Frances Press, 1990).
- [2] H. T. Kim, B. G. Chae, D. H. Youn, S. L. Maeng, G. Kim, K. Y. Kang, and Y. S. Lim, New J. Phys. **6**, 52 (2004).
- [3] H. T. Kim, K. Y. Kang, US patent 6,624,463, Priority: Sept. 2001
- [4] F. Chudnovski, S. Luryi, B. Spivak, "In Future Trends in Microelectronics: the Nano Millenium" (A. Zaslavsky. Ed., Wiley-Interscience, New York, 2002) pp148-155.
- [5] H. T. Kim, B. G. Chae, D. H. Youn, G. Kim, K. Y. Kang, and Y. S. Lim, Appl. Phys. Lett. **86**, 242101 (2005).
- [6] G. I. Petrov, V. V. Yakovlev and J. Squier, Appl. Phys. Lett. **81**, 1023 (2002).
- [7] S. Yamanouchi, Y. Taguchi and Y. Tokura, Phys. Rev. Lett. **83**, 5555 (1999).
- [8] H. Futaki and M. Aoki, Jpn. J. Appl. Phys. **8**, 1008 (1969).
- [9] J. C. Rakotoniaina, R. Mokrani-Tamellin, J. R. Gavarri, G. Vaquier, A. Casalot, and G. Calvarin, J. Solid State Chem. **103**, 81 (1993).
- [10] Y. Muraoka and Z. Hiroi, Appl. Phys. Lett. **80**, 583 (2002).
- [11] B. G. Chae, H. T. Kim, S. J. Yun, Y. W. Lee, B. J. Kim, D. H. Youn, and K. Y. Kang, Electrochem. Solid-State Lett. **9** C12 (2006).
- [12] W. F. Brinkman and T. M. Rice, Phys. Rev. B **2**, 4302 (1970).
- [13] H. T. Kim, Physica C **341-348** (2000) 259; 'New Trends in Superconductivity' NATO Science Series II Vol. **67** p137 (Eds, J. F. Annett and S. Kruchinin, Kluwer, 2002), cond-mat/0110112.
- [14] H. T. Kim, B. J. Kim, Y. W. Lee, B. G. Chae, S. J. Yun, K. Y. Kang, <http://xxx.lanl.gov/abs/cond-mat/0607577>.
- [15] A. Cavalleri, Cs. Toth, C.W. Siders, J.A. Squier, F. Raksi, P. Forget and J.C. Kieffer, Phys. Rev. Lett. **87**, 237401 (2001).
- [16] H. T. Kim, Y. W. Lee, B. J. Kim, B. G. Chae, S. J. Yun, K. Y. Kang, K. J. Han, K. Yee, and Y. S. Lim, <http://xxx.lanl.gov/abs/cond-mat/0608085>.
- [17] B. G. Chae, H. T. Kim, D. H. Youn and K. Y. Kang, Physica B **369**, 76 (2005).